Analysis of a Piezoelectric Sensor to Detect Flexural Waves

*[1]M. Veidt, [2]T. Liu and [2]S. Kitipornchai

[1]*Department of Mechanical Engineering, The University of Queensland, Brisbane, Qld. 4072, Australia*

[2]*Department of Civil Engineering, The University of Queensland, Brisbane, Qld. 4072, Australia*

ABSTRACT

In this paper the electro-mechanical transfer characteristics of adhesively bonded piezoelectric sensors are investigated. Using dynamic piezoelectricity theory, Mindlin plate theory for flexural wave propagation and a multiple integral transform method, the frequency response functions of piezoelectric sensors with and without backing materials are developed and the pressure-voltage transduction functions of the sensors calculated. The corresponding simulation results show that the sensitivity of the sensors is not only dependent on the sensors' inherent features such as piezoelectric properties and geometry, but also on local characteristics of the tested structures and the admittance and impedance of the attached electrical circuit. It is also demonstrated that the simplified rigid mass sensor model can be used to successfully analyse the sensitivity of the sensor at low frequencies, but that the dynamic piezoelectric continuum model has to be used for higher frequencies, especially around the resonance frequency of the coupled sensor-structure vibration system.

* corresponding author:
phone: +61 7 3365 3621
fax: +61 7 3365 4799
email: veidt@mech.uq.edu.au

INTRODUCTION

In the last decade an effective new approach for active control of structural vibrations has been developed and successfully applied to beam, plate and other types of structures, e.g. Fuller et. al.[1], Miller and Hall[2], Pan and Hansen[3] and Fujii et al.[4] It is based on the interpretation of the dynamic response of the structures in terms of travelling stress waves rather than the traditional vibration modal summation method. In this study, the wave sensing problem involved in these techniques is considered with the aim to quantify the electro-mechanical transduction characteristics and hence to improve the efficiency of the travelling wave control techniques.

Although travelling wave concepts have been used in the design of control architectures before[5], the wave sensing characteristics have not been studied in great detail, especially at higher frequencies and for composite structures. The common practice of employing standard accelerometers as output devices is, in fact, insufficient since due to wave scattering effects, the output voltage of the sensor is not only dependent on the characteristics of the sensor alone but also on the dynamic behaviour of the structure. Therefore, to enable the inclusion of high frequency components which arrive earlier and thus are essential to enable the design of optimised control systems the sensors need to be particularly designed according to the characteristics of the structure to be controlled. In this paper, the sensing characteristics of piezoelectric sensors to flexural waves in elastic plates are investigated. Using the dynamic theory of piezoelectricity, Mindlin plate wave motion theory and a multiple integral transform method, the influence of the sensors' inherent features such as piezoelectric properties and geometry, the tested structures and the attached electric circuit are examined.

FORMULATION OF THE PROBLEM

As shown in Fig. 1, a piezoelectric crystal disk with top and bottom surface electrodes is attached to an isotropic plate. It is used to detect incoming flexural waves generated by an arbitrary external disturbance. As illustrated in Fig. 2, the z_1-coordinate axis is parallel to the poling axis of the longitudinal transducer and directed normal to the upper, traction free, and lower, adhesively bonded, circular surfaces. The two electrodes are connected to an electronic measurement circuit of admittance Y.

In the following section the input-output transfer characteristics between the incoming flexural wave and the output voltage of the piezoelectric sensor are determined. In this investigation a dynamic one-dimensional piezoelectric model is used to approximate the electro-mechanical transduction characteristics of the piezoelectric sensor. This means that except for the extensional stress and the electric displacement along the thickness, all stress and electric displacement components in the piezoelectric disk vanish, either exactly or approximately. Thus, according to the linear theory of piezoelectricity[6,7] the following equations hold:

stress equation of motion
$$\frac{\partial T_{zz1}}{\partial z_1} = \rho_1 \frac{\partial^2 w_1}{\partial t^2}, \tag{1}$$

charge equation of electrostatics
$$\frac{\partial D_{z1}}{\partial z_1} = 0, \tag{2}$$

strain displacement relation
$$S_{zz1} = \frac{\partial w_1}{\partial z_1}, \tag{3}$$

quasi-static potential
$$E_{z1} = -\frac{\partial \phi}{\partial z_1}, \tag{4}$$

and the

piezoelectric constitutive relations
$$S_{zz1} = s_{33}^E T_{zz1} + d_{33} E_{z1}, \tag{5a}$$
$$D_{z1} = d_{33} T_{zz1} + \varepsilon_{33}^T E_{z1}, \tag{5b}$$

where t denotes time; $w_1(z_1)$, $S_{zz1}(z_1)$ and $T_{zz1}(z_1)$ are the mechanical displacement, strain and stress in the piezoelectric transducer, respectively; D_{z1}, E_{z1} and ϕ represent the electric displacement and electric potential in the z_1 direction and a scalar electric potential, respectively, and ρ_1, s_{33}^E, d_{33} and ε_{33}^T are the mass density, the elastic compliance, piezoelectric charge constant and dielectric constant of the piezoelectric sensor, respectively.

In previous investigations of the wave control techniques[1] the classical thin plate theory has been used to model the behaviour of the flexural waves. In order to accurately analyse the wave sensing characteristics of the piezoelectric crystal sensor the Mindlin plate theory is employed in this study. Thus, in the Cartesian coordinate system *(x,y,z)* with the *x*-and *y*-axes lying in the plane of the plate and its origin in the mid-plane of the plate as shown in Fig. 3, the propagation behaviour of the flexural waves is described by, e.g[8]

$$(\nabla^2 - \frac{\rho}{G'}\frac{\partial^2}{\partial t^2})(D\nabla^2 - \frac{\rho h^3}{12}\frac{\partial^2}{\partial t^2})w(x,y,t) + \rho h\frac{\partial^2 w(x,y,t)}{\partial t^2} =$$

$$(1 - \frac{D}{G'h}\nabla^2 + \frac{\rho h^2}{12G'}\frac{\partial^2}{\partial t^2})q(x,y,t) \tag{6}$$

in which

$$\nabla^2 = \frac{\partial^2}{\partial x^2} + \frac{\partial^2}{\partial y^2}, \tag{7a}$$

$$G' = k^2 G, \tag{7b}$$

$$D = \frac{Eh^3}{12(1-\nu^2)} \tag{7c}$$

where t is the time variable; $w(x,y,t)$ the transverse deflection of the plate; k^2 is a correction factor relating to Rayleigh surface waves given by $0.76+0.3\nu$; E, G, ν are Young's modulus, shear modulus and Poisson's ratio; ρ is the material density, h is the plate thickness and q the distributed forces exerted on the surface of the plate by external disturbances and the sensor.

DETERMINATION OF THE FREQUENCY RESPONSE FUNCTIONS (FRF) OF THE BONDED SENSOR

In the travelling wave control technique, the vibration behaviour of the structure whose dynamic response has to be optimised is characterised by the propagation behaviour of stress waves. In the case of small deformations and linear elasticity their motion can be readily analysed as the superposition of harmonic plane waves of different frequencies and different wave numbers. In the following paragraphs the sensing

characteristics of contact-type piezoelectric transducers used as sensors in the control loop are derived. As indicated in Fig.1, an arbitrary incident harmonic plane wave

$$w_{in}(x,y,t) = A_0 e^{i(\kappa_x x + \kappa_y y - \omega t)} \tag{8}$$

is assumed to propagate towards the sensor, where A_0 is an arbitrary amplitude constant, ω is the circular frequency, and κ_x and κ_y are wave numbers in the directions of x and y, respectively. It is obvious that w_{in} satisfies (6), i.e. the wave numbers κ_x and κ_y and the frequency ω must satisfy the dispersion equation of the plate, which can be easily obtained by substituting (8) into (6).

When the incident wave w_{in} arrives at the sensor, a scattered wave field w_{s} is generated by the sensor. The scattered wave field is introduced as

$$w_s(x,y,t) = \overline{w}_s(x,y,\omega) e^{-i\omega t} \tag{9}$$

where $\overline{w}_s(x,y,\omega)$ is an unknown function. Due to the electro-mechanical coupling, this mechanical disturbance will lead to an electrical output. In the following subsections, the electro-mechanical coupling characteristics of the sensor and the mechanical coupling between the sensor and the plate will be analysed to determine the electrical voltage output of the sensor as a function of the incident wave.

Analysis of the Sensor. The electro-mechanical coupling characteristics of the piezoelectric sensor are analysed applying dynamic piezoelectricity theory. Substituting (3) into (5a) and then substituting the resultant equation into (1) yields

$$\frac{1}{s_{33}^E}\frac{\partial^2 w_1}{\partial z_1^2} - \frac{d_{33}}{s_{33}^E}\frac{\partial E_{z1}}{\partial z_1} = \rho_1 \frac{\partial^2 w_1}{\partial t^2} \tag{10}$$

Similarly, substituting (3) into (5b) and then substituting the resultant expression into (2) yields

$$\frac{d_{33}}{s_{33}^E}\frac{\partial^2 w_1}{\partial z_1^2} + (\varepsilon_{33}^T - \frac{d_{33}^2}{s_{33}^E})\frac{\partial E_{z1}}{\partial z_1} = 0 \tag{11}$$

Eliminating the term E_{z1} in (10,11), the following equation of motion results

$$\overline{c}_{33}\frac{\partial^2 w_1}{\partial z_1^2} = \rho_1 \frac{\partial^2 w_1}{\partial t^2} \tag{12}$$

in which

$$\bar{c}_{33} = \frac{1}{s_{33}^E}(1+\chi^2) \text{ and } \chi^2 = \frac{d_{33}^2}{\varepsilon_{33}^T s_{33}^E - d_{33}^2} \tag{13a,b}$$

In addition, the following expressions for the other mechanical and electrical variables are derived:

By integrating (1) with respect to z_1 the stress variable $T_{zz1}(z_1)$ can be expressed as

$$T_{zz1} = \int \rho \frac{\partial^2 w_1^2}{\partial z_1^2} dz_1 \tag{14}$$

From (3) and (5a), the electric field can be evaluated as

$$E_{z1} = \frac{1}{d_{33}} \frac{\partial w_1}{\partial z_1} - \frac{s_{33}^E}{d_{33}} T_{zz1} \tag{15}$$

Substituting (5a) into (5b), and noting (3), the electric displacement can be expressed as

$$D_{z1} = \frac{d_{33}}{s_{33}^E} \frac{\partial w_1}{\partial z_1} + (\varepsilon_{33}^T - \frac{d_{33}^2}{s_{33}^E}) E_{z1} \tag{16}$$

The upper and lower electrode surfaces are considered to operate into a measurement circuit of admittance Y, as shown in Fig. 2. The electric current in the circuit can be obtained as

$$I = \frac{d}{dt} \int_A D_{z1} dA = YV \tag{17}$$

where A represents the area of the upper or lower electrode surface and the voltage V is given by a potential difference as

$$V = \Delta\phi = \phi\Big|_{z_1=h_1} - \phi\Big|_{z_1=0} \tag{18}$$

Integrating (4) with respect to z_1, the potential difference can be evaluated as

$$\Delta\phi = -\int_0^{h_1} E_{z1} dz_1 \tag{19}$$

In view of equations (14-19), it can be seen that by solving for the mechanical displacement $w_1(z_1)$ all the other system variables and specifically the output voltage V will be obtained accordingly.

Applying the Fourier transform defined as

$$\overline{g}(\omega) = \int_0^\infty g(t) e^{-i\omega t} dt \tag{20}$$

to (12) yields

$$\frac{\partial^2 \overline{w}_1}{\partial z_1^2} + c_1^2 \omega^2 \overline{w}_1 = 0 \tag{21}$$

where $c_1 = \sqrt{\rho_1 / \overline{c}_{33}}$.

From (21), the frequency domain solution of the displacement $w_1(z_1)$ or, in other words, the wave motion within the piezoelectric disk can be expressed as

$$\overline{w}_1 = A_1 e^{ic_1 \omega z_1} + B_1 e^{-ic_1 \omega z_1} \tag{22}$$

where $A_1(\omega)$ and $B_1(\omega)$ are currently still unknown. It is necessary to point out that since the wave motion within the piezoelectric disk is considered, the model can be used to analyse thick as well as thin sensors.

Applying the Fourier transform (20) to (14) and making use of (22), results in

$$\overline{T}_{zz1} = ic_1 \overline{c}_{33} \omega (A_1 e^{ic_1 \omega z_1} - B_1 e^{-ic_1 \omega z_1}) + \gamma_1 \tag{23}$$

where $\gamma_1(\omega)$ is unknown.

Similarly, applying the Fourier transform to (15), and noting (23), the frequency domain solution of the electric field can be expressed as

$$\overline{E}_{z1} = -\frac{i\omega c_1 \chi^2}{d_{33}} (A_1 e^{ic_1 \omega z_1} - B_1 e^{-ic_1 \omega z_1}) - \frac{s_{33}^E}{d_{33}} \gamma_1 \tag{24}$$

Applying the Fourier transform to (16) and then substituting (22,24) into the resultant equations, the frequency domain solution of the electric displacement is obtained

$$\overline{D}_{z1} = -\frac{d_{33}}{\chi^2} \gamma_1 \tag{25}$$

Applying the Fourier transform to (18,19) and using (24), the frequency domain solution of the output voltage of the sensor can be expressed as

$$\overline{V} = \frac{\chi^2}{d_{33}} (e^{ic_1 \omega h_1} - 1) A_1 + \frac{\chi^2}{d_{33}} (e^{-ic_1 \omega h_1} - 1) B_1 + \frac{s_{33}^E h_1}{d_{33}} \gamma_1 \tag{26}$$

In addition, the frequency domain solution of the output voltage of the sensor can be derived by applying the Fourier transform to (17) and using (25)

$$\overline{V} = \frac{id_{33}A\omega}{\chi^2 Y}\gamma_1 \tag{27}$$

Comparing (26) and (27), the $\gamma_1(\omega)$ can be expressed as

$$\gamma_1 = \mu_1[(e^{ic_1\omega h_1} - 1)A_1 + (e^{-ic_1\omega h_1} - 1)B_1] \tag{28}$$

in which $\mu_1(\omega)$ is given by

$$\mu_1 = \frac{\chi^2}{i\dfrac{d_{33}^2 A\omega}{\chi^2 Y} - s_{33}^E h_1} \tag{29}$$

Thus, the frequency domain solutions of all mechanical and electrical variables can be expressed as functions of the two unknowns $A_1(\omega)$ and $B_1(\omega)$. In order to obtain these two unknowns, the behaviour of the incident and scattered stress waves at the sensor location needs to be considered.

Mechanical Consideration of the Plate. In order to evaluate the scattered wave field in the plate due to the contact pressure exerted by the sensor, the wave field caused by a point source at the origin of a cylindrical coordinate system is considered first. In this case the distributed force is

$$q = \frac{\delta(r)}{2\pi r} f(t) \tag{30}$$

where $\delta(r)$ is the Dirac delta function, $f(t)$ is a time function and $r = (x^2 + y^2)^{1/2}$.

Based on (6) and (30) and using the Fourier-Hankel transform method[9,10], the frequency domain solution of the wave field is

$$\overline{w} = -\frac{\bar{f}(\omega)}{4\pi D\delta_2^2}\left\{g_2(\omega)K_0(\sqrt{\delta_2^2 - \delta_1^2}\,r) + \right.$$

$$\left. \frac{\pi}{2} g_1(\omega)\left[Y_0(\sqrt{\delta_1^2 + \delta_2^2}\,r) + iJ_0(\sqrt{\delta_1^2 + \delta_2^2}\,r)\right]\right\}, \qquad 0 < \omega < \omega_c; \tag{31a}$$

$$\overline{w} = -\frac{\bar{f}(\omega)}{4\pi D\delta_2^2}\frac{\pi}{2}\left\{g_1(\omega)Y_0(\sqrt{\delta_1^2 + \delta_2^2}\,r) - g_2(\omega)Y_0(\sqrt{\delta_1^2 - \delta_2^2}\,r) + \right.$$

$$\left. i\left[g_1(\omega)J_0(\sqrt{\delta_1^2 + \delta_2^2}\,r) - g_2(\omega)J_0(\sqrt{\delta_1^2 - \delta_2^2}\,r)\right]\right\}, \qquad \omega > \omega_c \tag{31b}$$

in which

$$g_1(\omega) = 1 - \left(\frac{\omega}{\omega_c}\right)^2 + \frac{c_p^2}{\omega_c^2}(\delta_1^2 + \delta_2^2), \tag{32a}$$

$$g_2(\omega) = 1 - \left(\frac{\omega}{\omega_c}\right)^2 + \frac{c_p^2}{\omega_c^2}(\delta_1^2 - \delta_2^2), \tag{32b}$$

$$\delta_1^2 = \frac{1}{2}\left(\frac{1}{c_p^2} + \frac{1}{k^2 c_s^2}\right)\omega^2, \tag{32c}$$

$$\delta_2^2 = \left[\frac{1}{4}\left(\frac{1}{c_p^2} - \frac{1}{k^2 c_s^2}\right)\omega^4 + \frac{1}{\alpha^2 c_p^2}\omega^2\right]^{1/2}, \tag{32d}$$

$$c_p = \sqrt{\frac{E}{\rho(1-\nu^2)}}, \quad c_s = \sqrt{\frac{G}{\rho}}, \quad \omega_c = \sqrt{\frac{12k^2 G}{\rho h^2}}, \quad \alpha^2 = \frac{h^2}{12} \tag{32e-h}$$

where $J_0(x)$ and $Y_0(x)$ are the Bessel functions of order zero of the first and second kind, and $K_0(x)$ is the modified Bessel function of the second kind of order zero[11].

Using the fundamental solution given above, the frequency domain solution of the scattered wave field in the plate due to the surface contact pressure exerted by the attached sensor can be obtained through integrating over the sensor contact area.

Considering the general equations for the scattered, (9), and incident wave field, (8), and using superposition principle the total wave field in the plate can be expressed as

$$w(x,y,t) = \overline{w}_s(x,y,\omega)e^{-i\omega t} + A_0 e^{i(\kappa_x x + \kappa_y y)}e^{-i\omega t} \tag{33}$$

In order to simplify the problem the following assumptions according to[12] are introduced: (1) the pressure distribution exerted by the sensor can be approximated with a piston distribution; (2) the contact area between the transducer and the plate is so small that the transducer displacement corresponds to the plate deflection at the centre of the contact area.

According to Fig. 2, the above assumptions and the traction free boundary condition at the upper surface of the sensor yield

$$T_{zz1} = 0, \quad \text{for } z_1 = 0, \tag{34a}$$

$$T_{zz1} = -p(t), \quad w_1 = w(0,0,t), \quad \text{for } z_1 = h_1 \tag{34b,c}$$

where $p(t)$ is the magnitude of the contact stress between the sensor and the plate.

In view of the harmonic character of the incident wave, the frequency domain expressions for equations (34a-c) are

$$\overline{T}_{zz1} = 0\,, \quad \text{for } z_1 = 0\,, \tag{35a}$$

$$\overline{T}_{zz1} = -\overline{p}(\omega)\,, \quad \text{for } z_1 = h_1\,, \tag{35b}$$

$$\overline{w}_1 = A_0 e^{i(\kappa_x x + \kappa_y y)} + H_{wp}\,\overline{p}(\omega)\,, \quad \text{for } z_1 = h_1 \tag{35c}$$

in which

$$H_{wp} = -\frac{1}{2D\delta_2^{\,2}} \int_0^a \Big\{ g_2(\omega) K_0(\sqrt{\delta_2^{\,2} - \delta_1^{\,2}}\, r_0) + \frac{\pi}{2} g_1(\omega) \Big[Y_0(\sqrt{\delta_1^{\,2} + \delta_2^{\,2}}\, r_0) + i J_0(\sqrt{\delta_1^{\,2} + \delta_2^{\,2}}\, r_0) \Big] \Big\} r_0 \, dr_0\,, \qquad 0 < \omega < \omega_c\,; \tag{36a}$$

$$H_{wp} = -\frac{\pi}{4D\delta_2^{\,2}} \int_0^a \Big\{ g_1(\omega) Y_0(\sqrt{\delta_1^{\,2} + \delta_2^{\,2}}\, r_0) - g_2(\omega) Y_0(\sqrt{\delta_1^{\,2} - \delta_2^{\,2}}\, r_0) + i \Big[g_1(\omega) J_0(\sqrt{\delta_1^{\,2} + \delta_2^{\,2}}\, r_0) - g_2(\omega) J_0(\sqrt{\delta_1^{\,2} - \delta_2^{\,2}}\, r_0) \Big] \Big\} r_0 \, dr_0\,, \qquad \omega > \omega_c \tag{36b}$$

where a is the radius of sensor. H_{wp} is obtained by using the fundamental solution (31a,b) and integrating all contributions of the uniformly distributed pressure $p(t)$ exerted by the sensor over the circular contact area. The subscript "wp" indicates that the pressure p causes the displacement w.

Solution of the FRF. Substituting (23) and (28) into (35a,b) and (22) into (35c), results in the following three equations

$$\Big[ic_1 \overline{c}_{33}\omega + \mu_1 (e^{ic_1\omega h_1} - 1) \Big] A_1 + \Big[-ic_1 \overline{c}_{33}\omega + \mu_1 (e^{-ic_1\omega h_1} - 1) \Big] B_1 = 0\,, \tag{37a}$$

$$\Big[ic_1 \overline{c}_{33}\omega e^{ic_1\omega h_1} + \mu_1 (e^{ic_1\omega h_1} - 1) \Big] A_1 + \Big[-ic_1 \overline{c}_{33}\omega e^{-ic_1\omega h_1} + \mu_1 (e^{-ic_1\omega h_1} - 1) \Big] B_1 = -\overline{p}\,, \tag{37b}$$

$$e^{ic_1\omega h_1} A_1 + e^{-ic_1\omega h_1} B_1 = A_0 e^{i(\kappa_x x + \kappa_y y)} + H_{wp}\,\overline{p} \tag{37c}$$

Solving for the three unknowns yields

$$A_1 = -\frac{\theta_{12}}{\theta_{11}\theta_{22} - \theta_{12}\theta_{21}} A_0 e^{i(\kappa_x x + \kappa_y y)}\,, \tag{38a}$$

$$B_1 = \frac{\theta_{11}}{\theta_{11}\theta_{22} - \theta_{12}\theta_{21}} A_0 e^{i(\kappa_x x + \kappa_y y)}\,, \tag{38b}$$

$$\bar{p} = \frac{\theta_{31}\theta_{12} - \theta_{32}\theta_{11}}{\theta_{11}\theta_{22} - \theta_{12}\theta_{21}} A_0 e^{i(\kappa_x x + \kappa_y y)} \tag{38c}$$

in which

$$\theta_{11} = ic_1\bar{c}_{33}\omega + \mu_1(e^{ic_1\omega h_1} - 1), \tag{39a}$$

$$\theta_{12} = -ic_1\bar{c}_{33}\omega + \mu_1(e^{-ic_1\omega h_1} - 1), \tag{39b}$$

$$\theta_{21} = e^{ic_1\omega h_1} + H_{wp}[ic_1\bar{c}_{33}\omega e^{ic_1\omega h_1} + \mu_1(e^{ic_1\omega h_1} - 1)], \tag{39c}$$

$$\theta_{22} = e^{-ic_1\omega h_1} + H_{wp}[-ic_1\bar{c}_{33}\omega e^{-ic_1\omega h_1} + \mu_1(e^{-ic_1\omega h_1} - 1)] \tag{39d}$$

$$\theta_{31} = ic_1\bar{c}_{33}\omega e^{ic_1\omega h_1} + \mu_1(e^{ic_1\omega h_1} - 1), \tag{39e}$$

$$\theta_{32} = -ic_1\bar{c}_{33}\omega e^{-ic_1\omega h_1} + \mu_1(e^{-ic_1\omega h_1} - 1) \tag{39f}$$

Substituting (38a,b) into (28), the unknown $\gamma_1(\omega)$ is obtained as

$$\gamma_1 = \frac{\theta_{12}(1 - e^{ic_1\omega h_1}) + \theta_{11}(e^{-ic_1\omega h_1} - 1)}{\theta_{11}\theta_{22} - \theta_{12}\theta_{21}} \mu_1 A_0 e^{i(\kappa_x x + \kappa_y y)} \tag{40}$$

Using (40), the frequency domain solution of the output of the sensor is obtained from (27) as

$$\bar{V} = H_{Vhin} A_0 e^{i(\kappa_x x + \kappa_y y)} \tag{41}$$

in which

$$H_{Vhin} = \frac{i\omega d_{33} A \mu_1}{\chi^2 Y} \frac{\theta_{12}(1 - e^{ic_1\omega h_1}) + \theta_{11}(e^{-ic_1\omega h_1} - 1)}{\theta_{11}\theta_{22} - \theta_{12}\theta_{21}} \tag{42}$$

where H_{Vhin} is the frequency response function of the output voltage V of the sensor to a harmonic incident wave with amplitude A_0 and circular frequency ω.

Additionally, using (41) and (38c), the voltage-pressure transduction function of the piezoelectric sensor is

$$T_{Vp} \equiv \frac{\bar{V}}{\bar{p}} = \frac{i\omega d_{33} A \mu_1}{\chi^2 Y} \frac{\theta_{12}(1 - e^{ic_1\omega h_1}) + \theta_{11}(e^{-ic_1\omega h_1} - 1)}{\theta_{31}\theta_{12} - \theta_{32}\theta_{11}} \tag{43}$$

It is important to note that this transduction function does not depend on the properties of the plate, whereas equation (42) shows that the sensor voltage frequency response function is not only dependent on the sensor's inherent features, but also on the admittance of the attached electrical circuit and the characteristics of the plate.

Resonance Frequencies To better understand the sensing characteristics of the piezoelectric transducer, the free vibration resonance frequencies of the sensor and the resonance frequency of the pressure-voltage transduction of the bonded sensor are discussed in the following paragraphs.

If the upper and lower surfaces of the sensor are considered to be stress free, (23) and (25) yield the eigenvalue equation $\sin(c_1 h_1 \omega) = 0$, i.e., the resonance frequencies of the free-free piezoelectric sensor are

$$\omega_0 = n\frac{\pi}{c_1 h_1}, \quad n=1,2,3,....., \text{ or} \tag{44a}$$

$$f_0 = \frac{\omega_0}{2\pi} = \frac{n}{2c_1 h_1}, \quad n=1,2,3,..... \tag{44b}$$

Using (43) the pressure-voltage transduction of the sensor when the impedance of the attached electrical circuit is very large or the admittance $Y \approx 0$ is

$$T_{Vp} = -\frac{\chi^2}{d_{33}}\frac{\sin(c_1 h_1 \omega / 2)}{\cos(c_1 h_1 \omega / 2)} \tag{45}$$

Therefore, the resonance frequencies are the roots of $\cos(c_1 h_1 \omega / 2) = 0$, i.e.,

$$\omega^* = (2n-1)\frac{\pi}{c_1 h_1}, \quad n=1,2,3,...., \text{ or} \tag{46a}$$

$$f^* = \frac{\omega^*}{2\pi} = \frac{2n-1}{2c_1 h_1}, \quad n=1,2,3,.... \tag{46b}$$

Comparing (44a,b) and (46a,b), it is observed that the free-free vibration resonance frequencies are not the same as the resonance frequencies of the pressure-voltage transduction of the sensor except for the first resonance frequency n=1. The relationship between the two can be expressed as

$$\omega^* = 2\omega_0 - \frac{\pi}{c_1 h_1}, \quad \text{or} \tag{47a}$$

$$f^* = 2f_0 - \frac{1}{2c_1 h_1} \tag{47b}$$

The existence of these two kinds of resonance frequencies and their relationship are important for understanding the sensing characteristics of the sensors at higher frequencies.

FREQUENCY RESPONSE FUNCTIONS OF A SENSOR WITH BACKING MATERIALS

In order to improve the sensitivity of an adhesively attached piezoelectric sensor, one may put some backing material on the upper surface of the sensor. In this section, the influence of the modification on the frequency response functions of sensors is investigated.

Consider a sensor with an isotropic backing material as shown in Fig. 3. It is obvious that apart from traction free boundary condition at the upper surface all equations for the sensor and the plate in the previous section are still valid. Referring to the coordinate system for the backing material as introduced in Fig. 3, we have the following additional equations corresponding to the equation of motion, the constitutive relation and the upper surface boundary condition of the backing material

$$\frac{\partial T_{zz2}}{\partial z_2} = \rho_2 \frac{\partial^2 w_2}{\partial t^2} \ , \tag{48}$$

$$T_{zz2} = E_2 \frac{\partial w_2}{\partial t} , \tag{49}$$

$$T_{zz2} = 0 , \quad \text{for } z_2 = 0 \tag{50}$$

where w_2 and T_{zz2} denote the displacement and stress components along the thickness direction of the backing material; ρ_2 and E_2 are the mass density and Young's modulus, respectively.

The previous free traction condition at the upper surface of the sensor (34b) is replaced by the following two displacement and stress continuity conditions

$$w_1 = w_2 , \quad \text{for } z_1 = 0 \text{ and } z_2 = h_2 , \tag{51a}$$

$$T_{zz1} = T_{zz2} , \quad \text{for } z_1 = 0 \text{ and } z_2 = h_2 \tag{51b}$$

Considering these additional and modified equations and applying a similar analysis procedure, the new frequency response function of the sensor with a backing material to a harmonic incident wave is obtained as

$$H_{Vhin} = \frac{i\omega d_{33} A \mu_1}{\chi^2 Y} \frac{\theta'_{12}(1 - e^{ic_1 \omega h_1}) + \theta'_{11}(e^{-ic_1 \omega h_1} - 1)}{\theta'_{11}\theta_{22} - \theta'_{12}\theta_{21}} \tag{52}$$

in which

$$\theta'_{11} = \theta_{11} + c_2 E_2 \omega \tan(c_2 h_2 \omega), \tag{53a}$$

$$\theta'_{12} = \theta_{12} + c_2 E_2 \omega \tan(c_2 h_2 \omega) \tag{53b}$$

It turns out that all the solutions for the case of a sensor without backing materials can be applied provided θ_{11} and θ_{12} as given in (39a,b) are replaced by the expressions given above. Thus, the pressure-voltage transduction function of a sensor with backing material can be written as

$$T_{Vp} \equiv \frac{\overline{V}}{\overline{p}} = \frac{i\omega d_{33} A \mu_1}{\chi^2 Y} \frac{\theta'_{12}(1 - e^{ic_1 \omega h_1}) + \theta'_{11}(e^{-ic_1 \omega h_1} - 1}{\theta_{31}\theta'_{12} - \theta_{32}\theta'_{11}} \tag{54}$$

NUMERICAL RESULTS AND DISCUSSION

In this section, the simulation results of the sensing characteristics of adhesively bonded piezoelectric sensors attached to an isotropic plate are presented. If not otherwise stated, the material parameters of the plate are ρ=2700 kg/m^3, E=71.7×10^9 N/m^2 and ν=0.33; the piezoelectric material characteristics are s_{33}^E=18.5×10^{-12} m^2/N, d_{33}=374×10^{-12} m/V, ε_{33}^T=15045×10^{-12} F/m and ρ_1=7700 kg/m^3; and the backing material is copper with ρ_2=8900 kg/m^3 and E_2=117.2×10^9 N/m^2.

In Fig. 4a, the influence of the thickness of the sensor is examined. Three sensors of different thickness (h_1=5mm, 3mm, 2mm) are considered. According to (44b), the first resonance frequencies of the free vibration for these three sensors are calculated to be f_0=0.376MHz, 0.626MHz and 0.94MHz and according to (32g) the cutoff frequency of the 2mm thick plate is 0.807MHz. Fig. 4a shows that the frequencies corresponding to the three peaks are 0.36MHz, 0.58MHz and 1.05MHz which do not correspond to any of the above special frequencies. This clearly demonstrates that the knowledge of the sensor's free vibration behaviour is not sufficient to accurately predict its frequency response characteristics when it is attached to a structure. Additionally, it is seen that, as expected, thicker sensors are more sensitive in the low frequency region, and their first resonance frequency is narrowband compared to thinner sensors.

In Fig. 4b, the results of the voltage frequency response function for sensors with different thickness are shown for frequencies below 100kHz. In this simulation the flexural waves are generated by a normal point force *s(t)*, which is located a distance

r_0=0.2m away from the sensor. The normal point force $s(t)$ can be an arbitrary function in time and the voltage frequency response function H_{Vin} is defined as the ratio of the voltage output frequency spectrum $\overline{V}$ to the normal point force input frequency spectrum $\overline{s}$. This modification has no influence on the character of the results compared to the case with a general harmonic wave input, which is used in all other simulations. But it represents a typical experimental configuration used to determine the frequency response function of piezoelectric sensors and therefore is better suited to be compared with experimental data, which may be found in the literature. The results show that even in the low frequency regime the thickness of the sensor has a significant influence on the sensitivity of the measurement system. This emphasises the relevance of the piezodynamic model since a conventional rigid sensor model[13] would not be able to predict these results and therefore the quantitative analysis of experimental results or the optimisation of a specific measurement configuration would not be possible.

In Fig. 5, the influence of the flexural stiffness of the structure is examined. It is observed that a thicker substrate results in a larger response amplitude but shows a narrow resonance peak compared to a thinner plate. This shows again that the complex sensor-substrate interaction processes dominate the overall behaviour of the measurement system and their knowledge is essential to enable the quantitative prediction of experimental observations and the optimisation of the measurement system.

Fig. 6 shows the influence of the admittance of the attached electrical circuit on the measurement system's performance. It turns out that its influence is restricted to a small frequency range around the resonance frequency. But it is important to note that it may have a pronounced influence on the system's sensitivity if the admittance becomes large, i.e. the sensor is coupled to an electrical circuit with low impedance.

In Fig. 7, the influence of copper backing on the sensor's voltage output is examined. As expected, the backing material has a significant influence on its sensitivity and frequency response. More resonance frequencies exist within a given frequency regime and the first resonances are shifted to lower frequencies. Therefore, by carefully choosing the backing material for a sensor attached to a specific structure it is possible to optimise the performance of the measurement system.

In order to simplify the analysis of a sensor's sensitivity to incoming flexural waves, the sensor has been modelled as a rigid disc before[13]. For the purposes of checking the validity of this simplified analysis method, the pressure sensed by a sensor is evaluated both by the rigid mass model and by the present elastic continuum model. The comparison of the two results for the case of a sensor with and without backing material are given in Figs. 8a and 8b, respectively. The results show that the two models are in good agreement away from the system's resonance frequencies. But since the rigid sensor model is not able to represent the wave reflections within the sensor, it is no longer valid around the resonance frequencies and should therefore be avoided to predict the sensor's characteristics especially for thicker sensors and sensors with backing materials.

CONCLUSIONS

The wave sensing problem for contact-type sensors used in the travelling wave control techniques has been investigated in this paper. Using the dynamic theory of piezoelectricity, Mindlin plate wave motion theory and a multiple integral transform method, the voltage output frequency response functions of piezoelectric sensors with and without backing materials adhesively attached to a plate to incoming flexural waves has been developed. The results of the numerical simulations have shown that:

(1) the sensitivity of a piezoelectric sensor attached to a structure not only depends on the properties of the sensor itself, but also on the characteristics of the tested structure and the admittance of the attached electric circuit. Hence, for maximum sensitivity of the travelling wave control technique, it is required to design the sensors according to the characteristics of the structure to be controlled, the electric characteristics of the attached measurement device and the frequency range of the external disturbance.

(2) adding a backing material to a piezoelectric sensing element is changing its frequency response characteristics especially in the low frequency regime. This may provide some additional flexibility to optimise the sensitivity of the measurement system. However, it also makes its behaviour more complicated since more resonance frequencies occur. Thus, backing materials need to be chosen properly by quantitative analysis to achieving maximum sensitivity in the frequency regime of interest.

(3) provided the admittance of the attached electric circuit is very small, i.e. its impedance is very large, its influence on the sensitivity of the sensor can be neglected.

(4) the simplified rigid mass model for a sensor can be used to characterise the sensitivity of the measurement system away from its resonance frequencies. But it is no longer valid around the resonance frequencies and should therefore be avoided to predict the sensor's characteristics especially for thicker sensors and sensors with backing materials.

ACKNOWLEDGMENT

This work has been supported by the Australian Research Council under Grant No. A89937136.

REFERENCES

[1]Fuller C. R., Elliott S. J. and Nelson, P. A., *Active Control of Vibration*. Academic Press, 1996.

[2]Miller, D. W. and Hall, S. R., "Experimental Results Using Active Control of Travelling Wave Power Flow," *Journal of Guidance, Control, and Dynamics*, Vol. 14, No. 2, 1991, pp. 350-359.

[3]Pan, X and Hansen, C. H., "The Effect of Error Sensor Location and Type on the Active Control of Beam Vibration," *Journal of Sound and Vibration*, Vol. 165, No. 3, 1993, pp. 497-510.

[4]Fujii, H. A., Nakajima, K. and Matsuda, K., "Wave Approach for Control of Orientation and Vibration of a Flexural Structure," *Journal of Guidance, Control, and Dynamics*, Vol. 19, No. 3, 1996, pp. 578-583.

[5]Prakah-Asante, K. O. and Craig K. C., "Active Control Wave-Type Vibration Energy for Improved Structural Reliability," *Applied Acoustics*, Vol. 46, No. 1, 1995, pp. 175-195.

[6]Tiersten,H. F., *Linear Piezoelectric Plate Vibrations*. New York, Plenum Press, 1969.

[7]Ristic, V. M., *Principles of Acoustic Devices*. New York, John Wiley & Sons, 1983.

[8]Miklowitz, J., "Flexural Stress Waves in an Infinite Elastic Plate Due to a Suddenly Applied Concentrated Transverse Load," *ASME Journal of Applied Mechanics*, Vol. 27, No. 4, 1960, pp. 681-689.

[9]Sneddon, I. N., *Fourier Transforms*. New York, McGraw-Hill Book Company, Inc, 1951.

[10]Miklowittz, J., *Elastic Waves and Waveguides*. New York, North-Holland Publishing Company Amsterdam, 1978.

[11]Gradshteyn, I. S. and Ryzhik, I. M., 1980, *Table of Integrals, Series, and Products,* Academic Press, New York.

[12]Williams, J. H., Karagulle, J. H. and Lee, S. S., "Ultrasonic Input-Output for Transmitting and Receiving Longitudinal Transducers Coupled to Same Face of Isotropic Elastic Plate," *Materials Evaluation*, Vol. 40, No. 6, 1982, pp. 655-662.

[13]Liu, T., Liew, K. M. and Kitipornchai, S., "Analysis of Acousto-Ultrasonic Characteristics for an Isotropic Thin plate," *Journal of Acoustical Society of America*, Vol.105, 1999, pp. 3318-3325.

FIGURE CAPTIONS

Fig. 1: A piezoelectric sensor adhesively attached to a plate for flexural wave detection

Fig. 2: Details of the piezoelectric sensor, some of the major electrical and mechanical model parameters and the local sensor coordinate system introduced

Fig. 3: Schematic of a piezoelectric sensor with backing material attached to a plate and coordinate systems used

Fig. 4a: The voltage frequency response function H_{Vin} of sensors with different thickness, plate thickness h=2mm, sensor diameter a=3mm, electrical admittance of measurement circuit $Y=10^{-7}$ 1/Ω

Fig. 4b: Low frequency regime of the voltage frequency response function $H_{Vin}=\overline{V}\,/\,\overline{s}$ of sensors with different thickness for a normal point force input, source-sensor distance r_0=0.2m, plate thickness h=2mm, sensor diameter a=3mm, electrical admittance of measurement circuit $Y=10^{-7}$ 1/Ω

Fig. 5: The voltage frequency response function H_{Vin} of a sensor attached to plates with different thickness, sensor thickness h_1=2mm, sensor diameter a=3mm, electrical admittance of measurement circuit $Y=10^{-7}$ 1/Ω

Fig. 6: The voltage frequency response function H_{Vin} of sensors attached to electrical circuits with different admittance, plate thickness h=2mm, sensor thickness h_1=2mm, sensor diameter a=3mm

Fig. 7: The voltage frequency response function H_{Vin} of sensors with copper backings of different thickness, plate thickness h=2mm, sensor thickness h_1=2mm, sensor diameter a=3mm, electrical admittance of measurement circuit $Y=10^{-7}$ 1/Ω

Fig. 8a: The frequency response function of the normalized contact pressure $\overline{p}\,/\,\overline{A}_0$ of two sensors of different thickness calculated by the present elastic continuum model and a simplified rigid sensor model, plate thickness h=2mm, sensor diameter a=3mm, electrical admittance of measurement circuit $Y=10^{-7}$ 1/Ω: a) without copper backing

Fig. 8b: The frequency response function of the normalized contact pressure $\bar{p}/\bar{A}_0$ of a sensor calculated by the present elastic continuum model and a simplified rigid sensor model, plate thickness h=2mm, sensor thickness h_1=1mm, sensor diameter a=3mm, electrical admittance of measurement circuit Y=10^{-7} 1/Ω: b) with copper backing, h_2=3mm

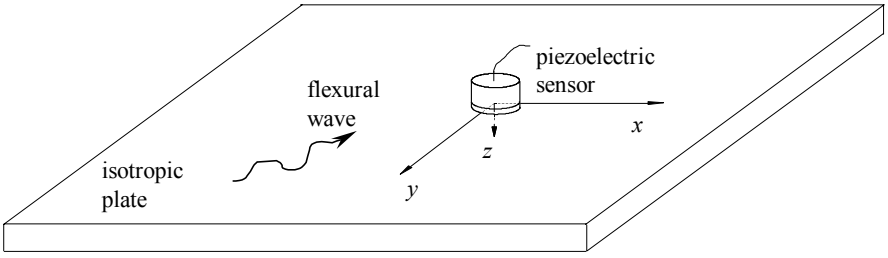

Fig. 1: A piezoelectric sensor adhesively attached to a plate for flexural wave detection

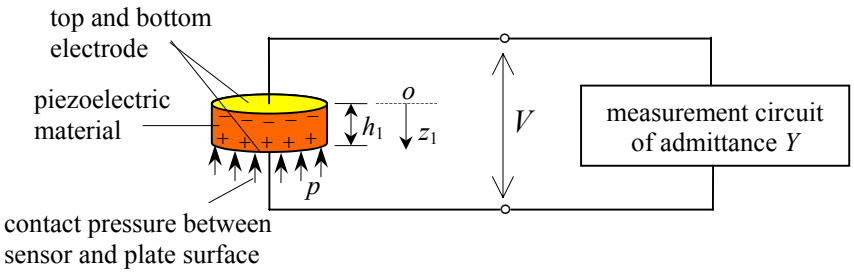

Fig. 2: Details of the piezoelectric sensor, some of the major electrical and mechanical model parameters and the local sensor coordinate system introduced

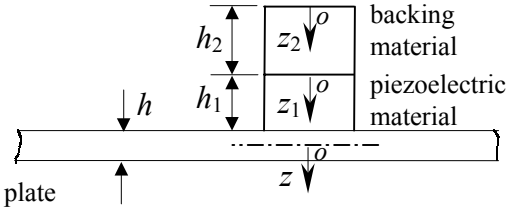

Fig. 3: Schematic of a piezoelectric sensor with backing material attached to a plate and coordinate systems used

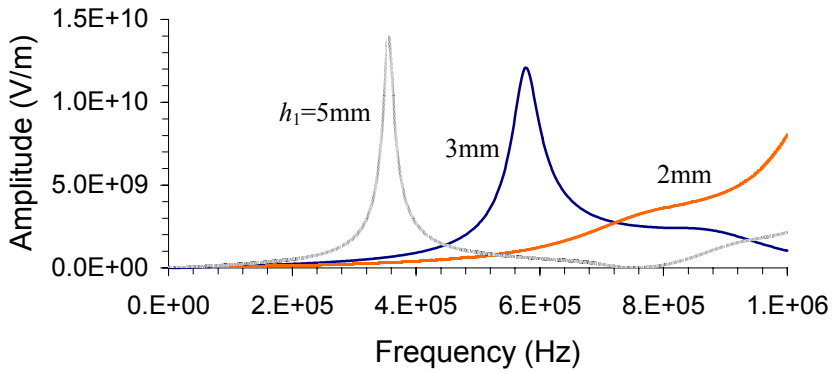

Fig. 4a: The voltage frequency response function H_{Vin} of sensors with different thickness, plate thickness h=2mm, sensor diameter a=3mm, electrical admittance of measurement circuit Y=10^{-7} 1/Ω

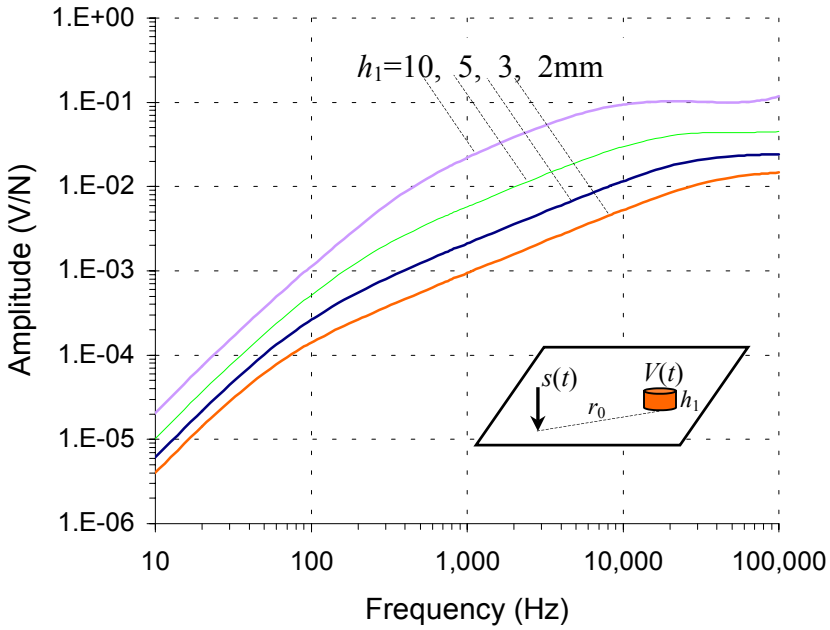

Fig. 4b: Low frequency regime of the voltage frequency response function $H_{Vin}=\overline{V}\,/\,\overline{s}$ of sensors with different thickness for a normal point force input, source-sensor distance r_0=0.2m, plate thickness h=2mm, sensor diameter a=3mm, electrical admittance of measurement circuit $Y=10^{-7}$ 1/Ω

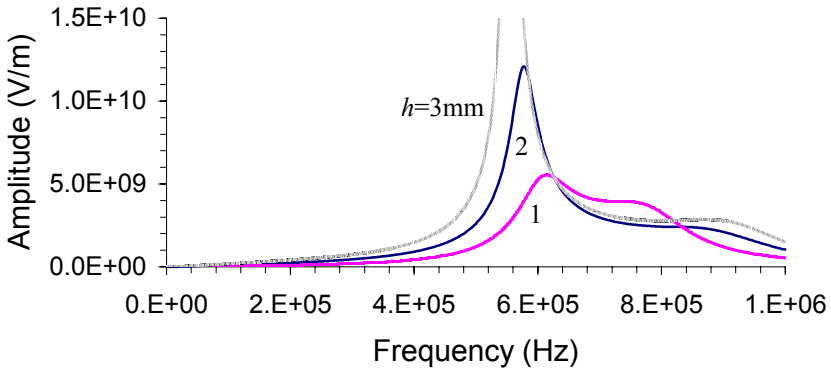

Fig. 5: The voltage frequency response function H_{Vin} of a sensor attached to plates with different thickness, sensor thickness h_1=2mm, sensor diameter a=3mm, electrical admittance of measurement circuit Y=10^{-7} 1/Ω

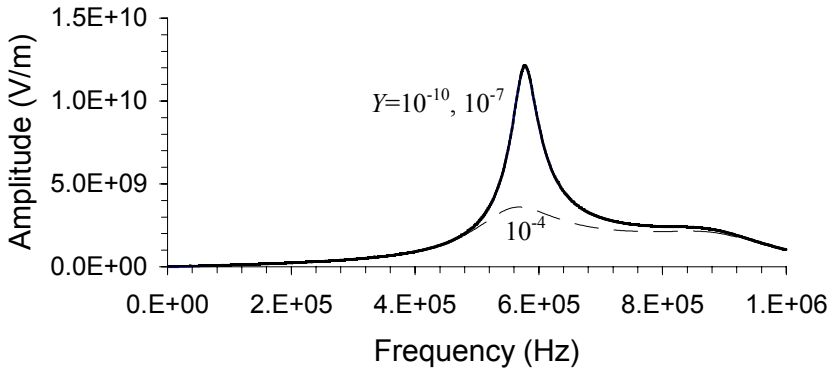

Fig. 6: The voltage frequency response function H_{Vin} of sensors attached to electrical circuits with different admittance, plate thickness h=2mm, sensor thickness h_1=2mm, sensor diameter a=3mm

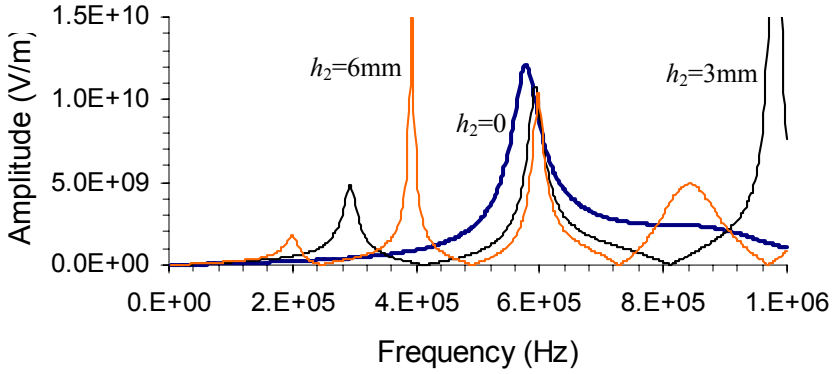

Fig. 7: The voltage frequency response function H_{Vin} of sensors with copper backings of different thickness, plate thickness h=2mm, sensor thickness h_1=2mm, sensor diameter a=3mm, electrical admittance of measurement circuit Y=10^{-7} 1/Ω

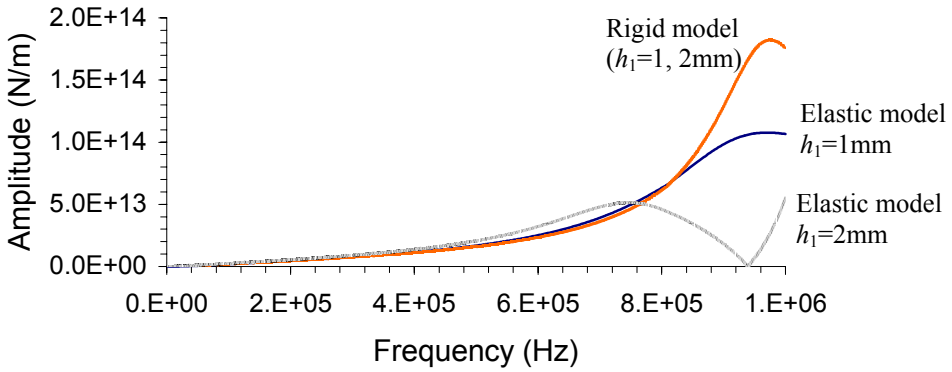

Fig. 8a: The frequency response function of the normalized contact pressure $\bar{p} / \bar{A}_0$ of two sensors of different thickness calculated by the present elastic continuum model and a simplified rigid sensor model, plate thickness h=2mm, sensor diameter a=3mm, electrical admittance of measurement circuit Y=10^{-7} 1/Ω: a) without copper backing

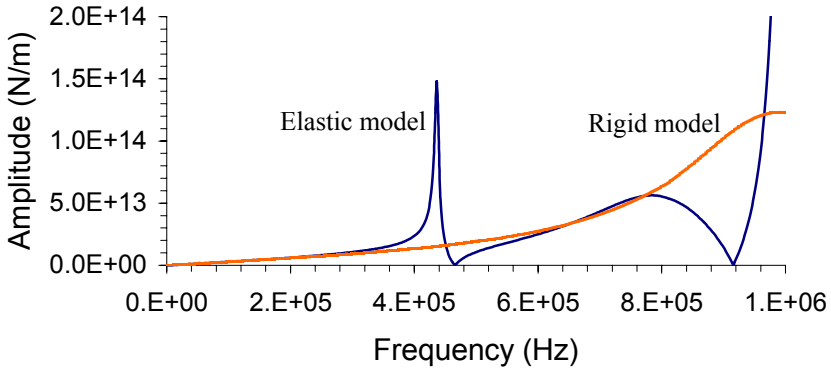

Fig. 8b: The frequency response function of the normalized contact pressure $\bar{p}/\bar{A}_0$ of a sensor calculated by the present elastic continuum model and a simplified rigid sensor model, plate thickness h=2mm, sensor thickness h_1=1mm, sensor diameter a=3mm, electrical admittance of measurement circuit Y=10^{-7} 1/Ω: b) with copper backing, h_2=3mm